

ExpertoCoder: Capturing Divergent Brain Regions Using Mixture of Regression Experts

Subba Reddy Oota¹

oota.subba@students.iiit.ac.in

Cognitive Science & Machine Learning Lab

¹IIIT-Hyderabad, India

Naresh Manwani¹

naresh.manwani@iiit.ac.in

Machine Learning Lab

¹IIIT-Hyderabad, India

Raju S. Bapi¹

raju.bapi@iiit.ac.in

Cognitive Science Lab

¹IIIT-Hyderabad, India

Keywords: fMRI Encoding, Mixture of Experts, Bayesian Brain

Abstract

fMRI semantic category understanding using linguistic encoding models attempts to learn a forward mapping that relates stimuli to the corresponding brain activation. Classical encoding models use linear multivariate methods to predict brain activation (all the voxels) given the stimulus. However, these methods mainly assume multiple regions as one vast uniform region or several independent regions, ignoring connections among them. In this paper, we present a mixture of experts model for predicting brain activity patterns. Given a new stimulus, the model predicts the entire brain activation as a weighted linear combination of activation of multiple experts. We argue that each expert captures activity patterns related to a particular region of interest (ROI) in the human brain. Thus, the utility of the proposed model is twofold. It not only accurately predicts the brain activation for a given stimulus, but it also reveals the level of activation of individual brain regions. Results of our experiments highlight the importance of the proposed model for predicting brain activation. This study also helps in understanding which of the brain regions get activated together, given a certain kind of stimulus. Importantly, we suggest that the mixture of regression experts (MoRE) framework successfully combines the two principles of organization of function in the brain, namely that of *specialization* and *integration*.

1 Introduction

fMRI measures the brain activity by identifying the changes in the blood-oxygen-level-dependent (BOLD) imaging signals in different functional areas in response to particu-

lar stimuli. In recent years, the use of both linear and non-linear multivariate encoding or decoding approaches for analyzing fMRI (functional magnetic resonance imaging) brain activity has become increasingly popular (Mitchell et al., 2008; Naselaris et al., 2011; Mesgarani et al., 2014; Di Liberto et al., 2015; Pereira et al., 2018). An encoding model that predicts brain activity in response to stimuli is essential for the neuroscience community, as the model predictions are useful to investigate and test hypotheses about the transformation from stimulus to brain responses both in the healthy brain and their breakdown in clinical conditions (Paninski et al., 2007; Kay et al., 2008; Dumoulin and Wandell, 2008; Yamins et al., 2014; Güçlü and van Gerven, 2017). Typically, experimental conditions utilize sensory, visual, motor, or auditory stimuli and so an encoding model maps the input stimuli to their encoding representation in the respective brain region (Kay et al., 2008; Mitchell et al., 2008; Dumoulin and Wandell, 2008; Pereira et al., 2018; Oota et al., 2019).

Understanding the association between the semantics of words/sentences and evoked brain activation may throw light on how the brain organizes and represents linguistic information through neural circuits. One of the pioneering works by Mitchell et al. (Mitchell et al., 2008) proposed distributional semantic models that encode patterns found in fMRI brain activation based on hand-designed features. Subsequently, models trained using word embedding have successfully overcome the limitations of manually-designed features to build encoding systems (Oota et al., 2018; Abnar et al., 2018; Pereira et al., 2018). Psycholinguistic and behavioral characteristics are also useful for the encoding task (Chang et al., 2011; Palatucci et al., 2009; Fernandino et al., 2015) and for visually-grounded representations (Anderson et al., 2017). These studies es-

establish a higher correlation between the semantic features and brain activation patterns. However, they do not have a principled way to predict regions which specialize in a particular category of stimuli. Instead, they predict the voxel intensity values either for the whole brain or for a pre-selected set of voxels.

Classical encoding models focus on univariate fMRI analysis, i.e., toward an understanding of different cognitive processes at individual brain voxels (Gonsalves and Cohen, 2010). Researchers have also explored multi-voxel pattern analysis (MVPA) (Mahmoudi et al., 2012) to represent the information across an ensemble of voxels. The critical limitation of MVPA is that it may detect areas where brain activation differs across subjects, even if those differences are unrelated to neural coding. Moreover, current encoding methods attempt to learn either weights in case of linear models (Mitchell et al., 2008; Pereira et al., 2018) or complex representations in non-linear models (Oota et al., 2018). Recent studies show that deep learning models (e.g., convolution neural networks and LSTMs) are successful in encoding brain responses for various sensory inputs (audio, visual and language) (Wen et al., 2018; Han et al., 2018; Rowtula et al., 2018; Wen et al., 2017; Oota et al., 2019). However, it remains unclear whether and to what extent the deep learning models can explain and encode stimuli to brain responses. Moreover, all these models vary in their complexity. In particular, interpretation of these non-linear models can be difficult due to unexpected and enigmatic representations (Benjamin et al., 2017; Kording et al., 2018).

In literature, empirical studies and many applications in neuroscience verify that both linear and non-linear methods outperform for a particular problem or a specific subset of input data, but it is incongruous to get a single global model achieving the best

results on the complete problem domain (Dietterich, 2000). Two fundamental principles of organization of function in the brain seem to be *functional differentiation* (specialization) and *functional integration* (Friston, 2002). Extant linear and non-linear models tend to conform to the latter principle by modeling the integrative aspect in a single global model. However, we hypothesize that such integration is mediated in turn by regional functional specialization. Such a framework posits that information organization in the brain is achieved holistically by combining the principles of differentiation and integration. A machine learning framework that elegantly combines these principles is the *mixture of experts* model (Jordan and Xu, 1995).

Mixture of Experts (MoE) models (Jordan and Xu, 1995) offer an exciting choice for the problem of learning distinct models for different regions of the input space. MoE has been used successfully to investigate the intricate patterns of brain changes associated with non-pathological and pathological processes, such as the effects of growth, aging, injury, or a disease (Kim et al., 2010; Eavani et al., 2016). Models involving MoEs have great potential for use in medical diagnostics to diagnose a variety of clinical conditions such as depression, Alzheimers' dementia. Yao et al. (Yao et al., 2009) proposed a Hidden Conditional Random Field (HCRF) framework in combination with a mixture of experts model to make predictions in all ROIs that are interconnected.

MoE model assumes that each expert specializes over a particular brain region (set of voxels that are significantly activated) based on the category of words that are represented by the model. Encoding models have proven to be successful that use pre-trained word embedding methods such as Word2Vec and GloVe to predict brain responses (Mikolov et al., 2013; Pennington et al., 2014). Here, we use Bidirectional

Encoder Representations from Transformers (BERT) embeddings (Devlin et al., 2018) to generate a feature vector for input stimuli. Finally, we modeled the fMRI signals as a linear combination of all expert predictions corresponding to the gate probabilities of each expert. We conducted simulation experiments showing that functional differentiation into divergent brain regions achieved with the mixture of regression experts rather than using a simple linear/non-linear model alone.

In summary, we make the following contributions in this paper.

- (i) A mixture of experts based model where a group of experts captures brain activity patterns related to particular regions of interest (ROI),
- (ii) In particular, we focus on categorizing different brain regions associated with different experts, given input stimuli.
- (iii) Showcase and highlight the importance of discrimination across different experts.
- (iv) Match the accuracy of the proposed model to that achieved by existing linear and non-linear models, thereby demonstrating the functional integration capability of such mixture models.

The rest of this paper is organized as follows. We discuss the proposed mixture of regression experts (MoRE) approach in Section 3, and our enhancements include a detailed analysis of the dataset, insights from analysis of results and discussion in Section 4, 5. Finally, we conclude with a summary in Section 6.

2 Motivation for Using Mixture of Experts

In Mixture of experts, the feature space probabilistically divided into several partitions. Every expert specializes in a distinct partition. The stimuli used in task-specific fMRI datasets arise from multiple categories of data and yield activation in different brain regions. The main objective of this paper is to demonstrate the feasibility of extracting brain activity patterns related to particular regions of specialization using a mixture of regression experts-based model (we call, *ExpertoCoder*) while maintaining comparable accuracy to that of integrative global models.

3 fMRI Encoding: Mixture of Regression Experts (MoRE)

Approach

We use a mixture of experts-based encoder model, whose architecture is inspired from (Jordan and Xu, 1995). The mixture of experts architecture is composed of a gating network and several expert networks, each of which solves a function approximation problem over a local region of the input space. Figure 1 shows an overview of our model where the input is text vector extracted from popular pre-trained neural word embedding model BERT (Devlin et al., 2018). The input feature representations passed through both the expert networks and the gating network. The gating network uses a probabilistic model to choose the best expert for a given input vector. The corresponding brain activation (for all the voxels) used as a target vector during training. As a result of training, the model learns to select appropriate expert via gating parameters in order to predict the whole brain activation for a particular stimulus. Also, the model highlights the spe-

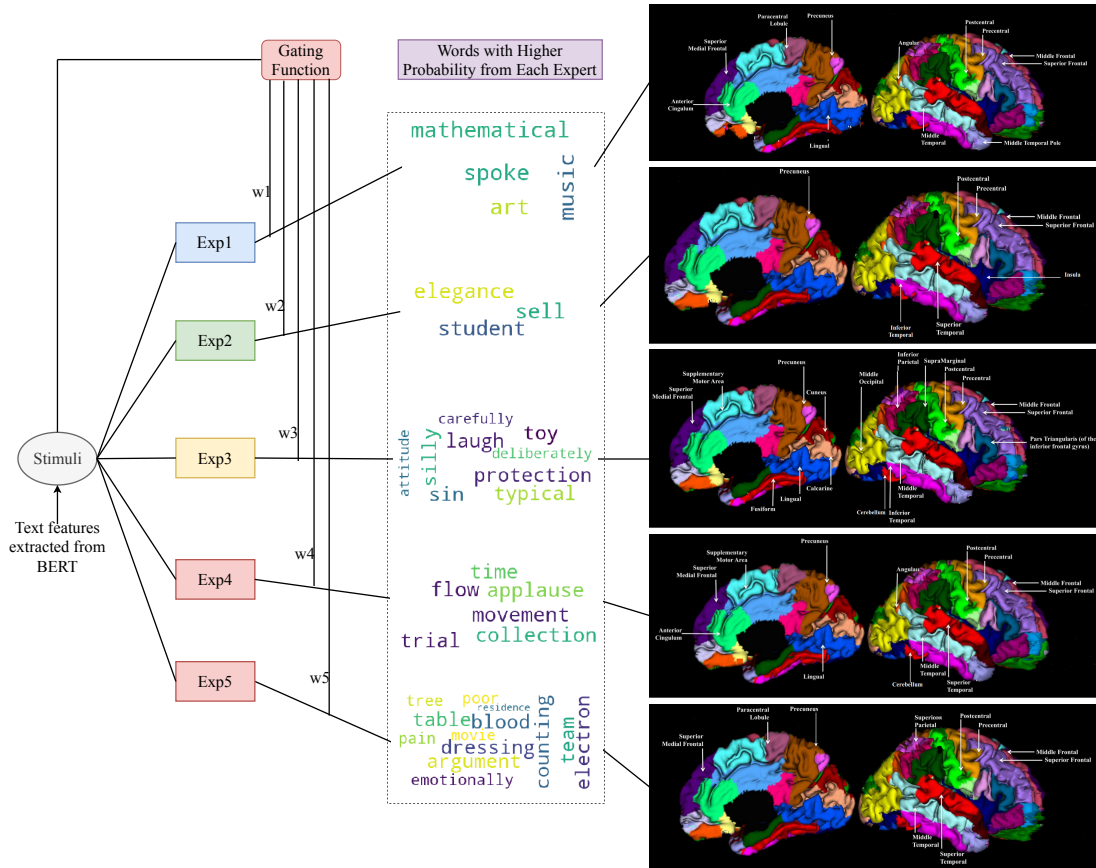


Figure 1: MoRE Architecture

cific activated brain regions for a particular stimulus. A similar architecture is used to build models for the subjects; however, a distinct model constructed for each subject. In the experiments and results section, we provide an in-depth analysis of the model hyperparameters and training.

3.1 Architecture:

Let $S = \{(\mathbf{x}_1, \mathbf{y}_1), \dots, (\mathbf{x}_N, \mathbf{y}_N)\}$ denote the training set where N is the number of examples. $\mathbf{x}_i \in \mathbb{R}^n$, $\forall i \in [N]$ are the input vectors (word embeddings). $\mathbf{y}_i \in \mathbb{R}^m$, $\forall i \in [N]$ are the target vectors (whole brain activation all the voxels in the fMRI images). Let K be the number of experts. The mixtures of experts model formulates the conditional

density of \mathbf{y} given \mathbf{x} as a mixture of K different densities as follows.

$$p(\mathbf{y}|\mathbf{x}) = \sum_{j=1}^K P(j|\mathbf{x}, \theta_0) p(\mathbf{y}|\mathbf{x}, \theta_j) = \sum_{j=1}^K g_j(\mathbf{x}, \theta_0) p(\mathbf{y}|\mathbf{x}, \theta_j) \quad (1)$$

Here, $P(j|\mathbf{x}, \theta_0) = g_j(\mathbf{x}, \theta_0)$ is the probability of choosing j^{th} expert for a given \mathbf{x} . Note that $\sum_{j=1}^K g_j(\mathbf{x}, \theta_0) = 1$ and $g_j(\mathbf{x}, \theta_0) \geq 0, \forall j \in [K]$. $g_j(\mathbf{x}, \theta_0)$ is also called the *gating function* and is parameterized by θ_0 . $p(\mathbf{y}|\mathbf{x}, \theta_j)$ denotes the density function for the output vector associated with the j^{th} expert and θ_j denotes the parameters associated with the j^{th} expert.

In this paper, we choose $p(\mathbf{y}|\mathbf{x}, \theta_j)$ as multivariate Gaussian probability density for each of the experts, denoted by:

$$p(\mathbf{y}|\mathbf{x}, W_j, \Sigma_j) = \frac{1}{(2\pi)^{m/2} |\Sigma_j|^{1/2}} \exp\left(-\frac{1}{2}(\mathbf{y} - W_j \mathbf{x})^T \Sigma_j^{-1} (\mathbf{y} - W_j \mathbf{x})\right) \quad (2)$$

where $W_j \in \mathbb{R}^{m \times n}$ is the weight matrix and $\Sigma_j \in \mathbb{R}^{m \times m}$ is the variance-covariance matrix associated with the j^{th} expert. Thus, $\theta_j = \{W_j, \Sigma_j\}$. In this formulation we assume that the variance-covariance matrix Σ_j is diagonal. That is, $\Sigma_j = \text{diag}(\sigma_{j,1}^2, \sigma_{j,2}^2, \dots, \sigma_{j,m}^2), \forall j \in [K]$. Thus, we assume that the components of the output vector $\mathbf{y} \in \mathbb{R}^m$ are statistically independent of each another. We use this assumption to make the model simple by reducing the number of overall parameters. This assumption also makes the algorithm computationally less expensive.

Assuming $\Sigma_j = \text{diag}(\sigma_{j,1}^2, \sigma_{j,2}^2, \dots, \sigma_{j,m}^2)$, we rewrite the conditional probability density model for j^{th} expert as follows:

$$P(\mathbf{y}|\mathbf{x}, W_j, \Sigma_j) = \frac{1}{(2\pi)^{m/2} \sigma_{j,1} \sigma_{j,2} \dots \sigma_{j,m}} \exp\left(-\sum_{i=1}^m \frac{(y_i - \mathbf{w}_{j,i}^T \mathbf{x})^2}{2\sigma_{j,i}^2}\right)$$

where $\mathbf{w}_{j,i}$ is the i^{th} row of W_j .

We use softmax function for the gating variable $g_j(\mathbf{x}, \theta_0)$.

$$g_j(\mathbf{x}, \theta_0) = \frac{\exp(\mathbf{v}_j^T \mathbf{x})}{\sum_{i=1}^K \exp(\mathbf{v}_i^T \mathbf{x})}$$

where $\mathbf{v}_j \in \mathbb{R}^n$, $\forall j \in [K]$. Thus, $\theta_0 = \{\mathbf{v}_1, \dots, \mathbf{v}_K\}$. Let Θ be the set of all the parameters involved for the K-experts. Thus, $\Theta = \{\theta_0, (W_1, \Sigma_1), \dots, (W_K, \Sigma_K)\}$.

3.2 Training Mixture of Experts Using Expectation Maximization

(EM) Algorithm

The EM algorithm is an iterative method for finding the maximum likelihood estimate (MLE) of the parameters of a probability model.

E-Step

In the E-step, we find the expectation of the complete log-likelihood.

$$Q(\Theta|\Theta^{(p)}) = \sum_{n=1}^N \sum_{j=1}^K h_j^{(p)}(\mathbf{x}_n) [\log(g_j(\mathbf{x}_n, \theta_0)) + \log(P(\mathbf{y}_n|\mathbf{x}_n, W_j, \Sigma_j))] \quad (3)$$

where p is the iteration index and $h_j^{(p)}(\mathbf{x}_n)$ is given by

$$h_j^{(p)}(\mathbf{x}_n) = \frac{g_j(\mathbf{x}_n, \theta_0^{(p)})P(\mathbf{y}_n|\mathbf{x}_n, W_j^{(p)}, \Sigma_j^{(p)})}{\sum_{i=1}^K g_i(\mathbf{x}_n, \theta_0^{(p)})P(\mathbf{y}_n|\mathbf{x}_n, W_i^{(p)}, \Sigma_i^{(p)})}$$

M-Step

The M step chooses a parameter Θ that maximizes Q function (given in eq.(3)). Thus,

$$\Theta^{(p+1)} = \underset{\Theta}{\operatorname{argmax}} Q(\Theta|\Theta^{(p)})$$

1. **Updating θ_0 :** We use gradient ascent to maximize Q function with respect to parameters θ_0 as there does not exist any closed-form solution for the maximizer.

$$\begin{aligned}\mathbf{v}_j^{(p+1)} &= \mathbf{v}_j^{(p)} + \eta \nabla_{\mathbf{v}_j} Q(\Theta | \Theta^{(p)}) \\ &= \mathbf{v}_j^{(p)} + \eta \sum_{n=1}^N [h_j^{(p)}(\mathbf{x}_n) - g_j(\mathbf{x}_n, \theta_0^{(p)})] \mathbf{x}_n\end{aligned}$$

where η is the step size.

2. **Updating W_j :** W_j comprises m rows $\mathbf{w}_{j,i}$. We derived the closed-form solution for $\mathbf{w}_{j,i}^{(p+1)}$ as follows:

$$\mathbf{w}_{j,i}^{(p+1)} = \left[\sum_{n=1}^N h_j^{(p)}(\mathbf{x}_n) \mathbf{x}_n \mathbf{x}_n^T \right]^{-1} \left[\sum_{n=1}^N h_j^{(p)}(\mathbf{x}_n) y_{n,i} \mathbf{x}_n \right], \quad j \in [K]; \quad i \in [m]$$

where $y_{n,i}$ is the i^{th} element of \mathbf{y}_n .

3. **Updating Σ_j :** Σ_j comprises $\sigma_{j,1}, \dots, \sigma_{j,m}$. We derived the closed-form update equation for each of them as follows:

$$\sigma_{j,i}^{(p+1)} = \frac{1}{\sum_{n=1}^N h_j^{(p)}(\mathbf{x}_n)} \sum_{n=1}^N h_j^{(p)}(\mathbf{x}_n) (y_{n,i} - \mathbf{w}_{j,i}^{(p)} \cdot \mathbf{x}_n)^2, \quad j \in [K]; \quad i \in [m]$$

An iteration of EM increases the original log-likelihood $L(\Theta | \mathbf{y}_1, \dots, \mathbf{y}_N)$. That is, $L(\Theta^{(p+1)} | \mathbf{y}_1, \dots, \mathbf{y}_N) > L(\Theta^{(p)} | \mathbf{y}_1, \dots, \mathbf{y}_N)$. The likelihood L increases monotonically along the sequence of parameter estimates generated by the EM algorithm.

3.3 Selection of Number of Experts

To find the number of experts, we used Bayesian Information Criterion (BIC) which is one of the successful measures to approximate the Bayes factor (Kass and Raftery, 1995), i.e., to find a model that has maximum posterior probability or maximum marginal

likelihood as well as a minimum number of model parameters. BIC can be formulated as follows.

$$BIC = d \log(N) - 2 \log(L(\Theta | \mathbf{y}_1, \dots, \mathbf{y}_N))$$

Where d is the number of parameters, N is the number of data points. The objective is to find a model configuration that minimizes BIC. The model complexity increases with the increase in the number of parameters. However, the likelihood will also increase by increasing complexity. Thus, BIC makes a trade-off between the negative likelihood and the number of parameters. There exists an optimal choice of complexity (number of experts here) at which BIC takes minimum value.

4 Experiments

This section organized as follows. We describe the datasets used for training and testing. In the next section, we present the process of selecting an appropriate number of experts in a model. In the subsequent section, we describe two exploratory experiments to investigate the nature of the semantic relatedness among the stimulus data and the related brain response data.

4.1 Dataset

We used data from paradigm 1 of fMRI experiment 1 (Pereira et al., 2018), where authors conducted experiments with multiple subjects by showing different categories of words as stimuli (images adapted from¹) as shown in Figure 2. Each category might

¹<https://osf.io/crwz7>



Figure 2: Examples of stimuli used for sample words (a noun, a verb, and an adjective) in experiment 1. Each word along with an image presented in multiple repetitions, and these images were adapted from (Pereira et al., 2018)

correspond to activation of distinct brain regions. In paradigm 1, the target word with a picture presented that depicted some aspect(s) of the relevant meaning. This fMRI dataset collected from a total of 17 participants. For each participant in the experiment, a whole set of 180 words (128 nouns, 22 verbs, 29 adjectives and adverbs, and one function word) as stimuli in the linguistic form used. The fMRI dataset constitutes of each image size 88×128 arranged as 85 slices, per subject per stimulus. We use the publicly available pre-trained word embedding method BERT (Devlin et al., 2018) to formulate feature vectors of 180 words as input and the corresponding brain responses of each participant (containing 200,000 voxels) as output to train the subject-specific model. Here, we use BERT-base embeddings, which yield 786-dimensional vector for each word. We use the Automated Anatomical Labeling (AAL) atlas (Craddock et al., 2012) with a parcellation of 116 brain regions to represent the brain activation response for each stimulus, where each voxel coordinate belongs to a particular region of interest.

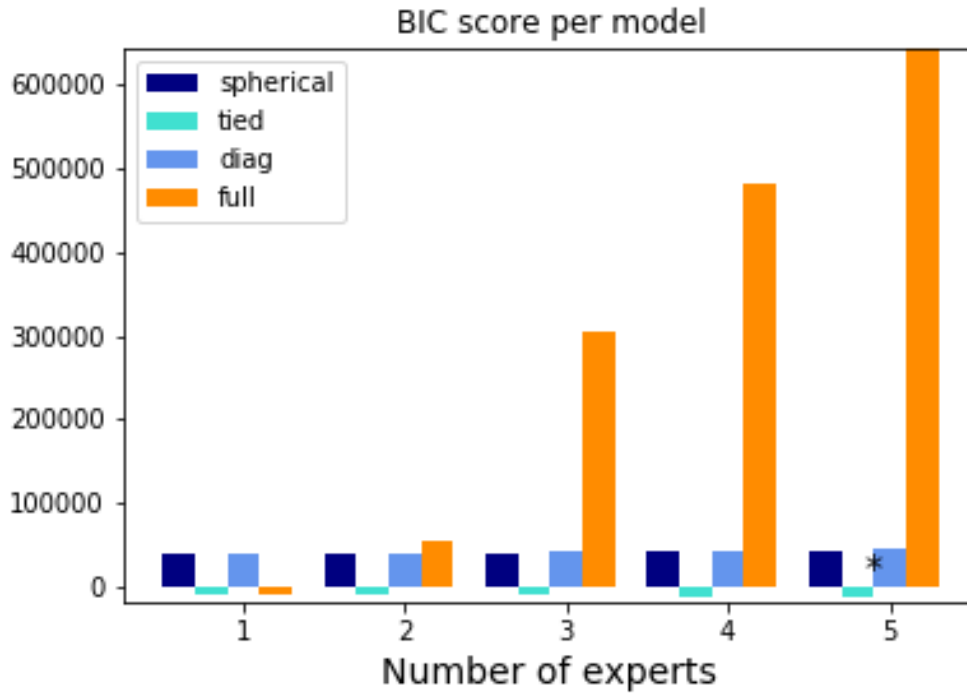


Figure 3: Selection of Number of Experts using Bayesian Information Criterion (BIC)

4.2 Choosing the Number of Experts:

As shown in Figure 3, we calculated the BIC scores using four different types of covariance parameters such as (1) ‘full’: each mixture component has its general covariance matrix, (2) ‘tied’: all components share the same general covariance matrix, (3) ‘diag’: own diagonal covariance matrix for each component, and (4) ‘spherical’: each component has its unique variance. The results showcase in Figure 3 corresponds to one subject where we can observe the optimal number of experts 5 with minimum BIC we wish to use. Across all the 17-subjects, we observe a similar number of experts.

4.3 Semantic Relatedness of the Stimulus Word Vectors

We characterize the semantic relatedness of the words used as stimuli by performing clustering of 180-word stimuli (features extracted from BERT). As seen in the word-cloud visualization in Figure 4, related words tend to appear together. These word clusters provide insight into how some words are highly correlated when cosine similarity (or correlation) measure was used to investigate semantic relatedness among the word-embedding vectors. We chose the number of clusters using the BIC method described above. From Figure 4, we observe that semantic word pairs such as (“smiling” & “laugh”), (“food & dinner”), (“job” & “business”), and (“camera” & “picture”) are grouped together in Cluster 1. Similarly in Cluster 2, we have (“mathematical”, “science”, & “economy”), (“election” & “nation”), (“king” & “war”), etc. Although, we often find similar pairs in the same cluster, we also find few uncorrelated words in every cluster.

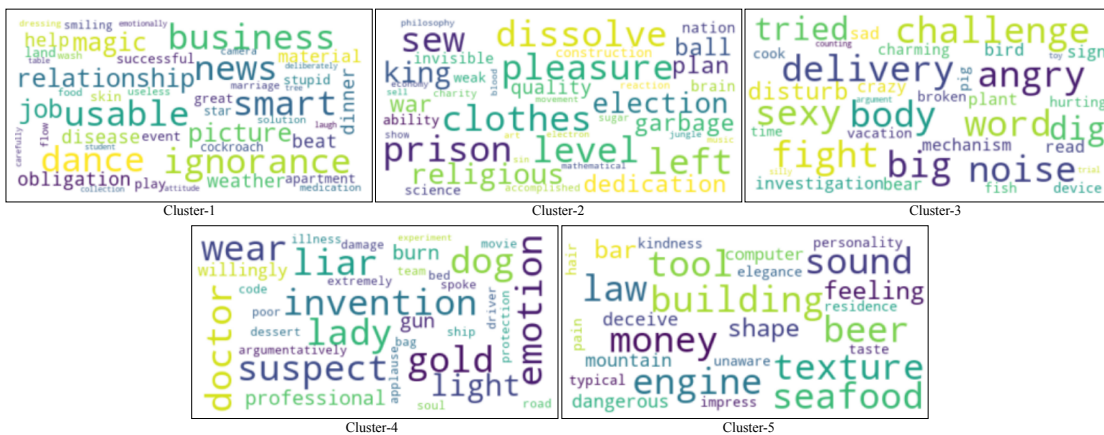


Figure 4: Visualization of the 180 target words (BERT embeddings) grouped into 5 clusters based on Cosine Similarity

4.4 Clustering of the fMRI Brain Activation Vectors

Understanding of how the brain represents semantics is still in its relative infancy: there are hypotheses no clearly articulated about how concepts are represented and combined. Here, we performed clustering of the fMRI brain activation vectors corresponding to the 180 stimulus words, and the results are as shown in Figure 5. We chose the number of clusters using the BIC method described above. From Figure 5, we can observe that words “body” and “brain” fall in the Cluster 1 whereas the word “skin” falls in Cluster 2. This result indicates that the semantic representations reflected in the brain activity might depend on the nature of the input stimuli that are shown to the subject and further might be related to how the subject responds to the image and word combination with his/her imagination and personal experience. Moreover, if we observe from Figure 2, the image is shown for the word “Plant” looks ambiguous. The subject might be thinking of this as “seed/s” that might in future become a plant and hence the corresponding brain activation might include all of these innate responses. This exploratory analysis suggests that although clusters may be formed based on similar semantic representations, however, each cluster may contain both correlated and uncorrelated words. Figure 6 shows the similarity (correlation) matrix among 180 brain activation vectors corresponding to the word stimuli, averaged across subjects. We observe high correlation again among similar words but also few unrelated words with high correlation, pointing to the variability in brain response when stimulated with lexical word and the visual stimulation by a corresponding image.

In the next section, we present the results of the proposed MoRE models, as to how they learn the associative relationships among the word embeddings and the related

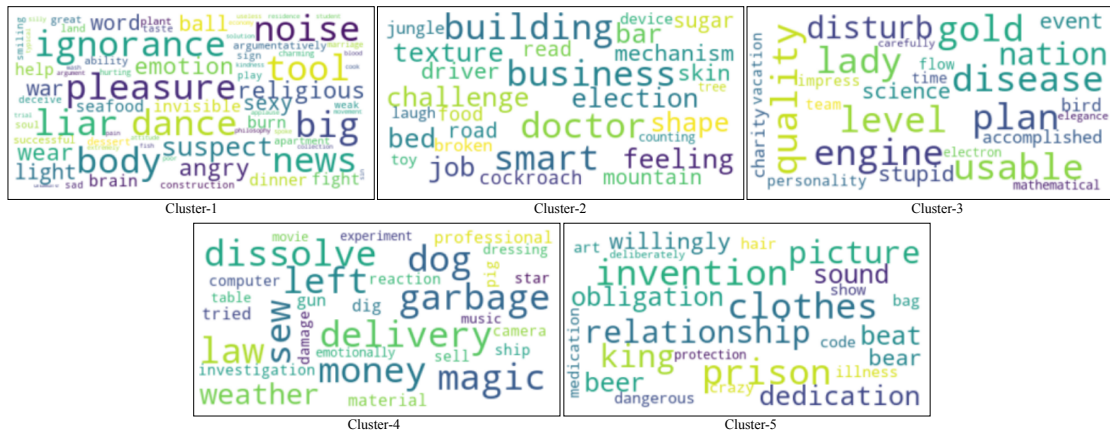


Figure 5: Visualization of the clusters formed when 180 brain activation responses are corresponding to the word stimuli grouped into 5 clusters.

brain activation responses.

5 Results and Discussion

Using the approach discussed in Section 3, we trained a separate mixture of regression experts (MoRE) model for each subject. We performed experiments on the dataset where the stimulus (text) vector extracted from the recently successful neural word-embedding method, namely, BERT, was given as input to the model and estimated the corresponding brain activation response as the output of the model. Specifically, we obtained a 768-dimensional vector using BERT embedding. We split the stimulus words into 144 words used in training and the remaining 36 words as the testing set. The encoding performance was evaluated by training and testing models using different subsets of the 180 words in a 5-fold cross-validation scheme. The encoder models were trained until the model reached convergence with a lower bound of $1e^{-10}$ or till a

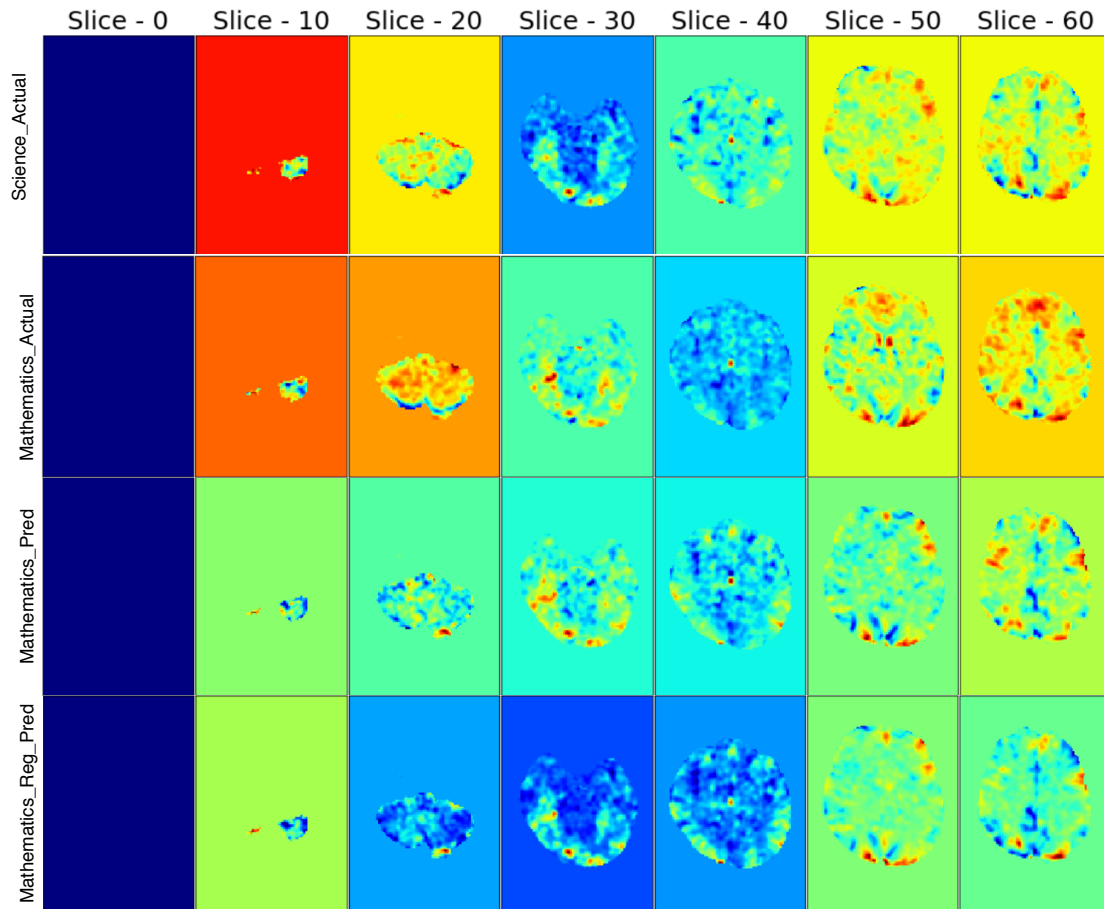
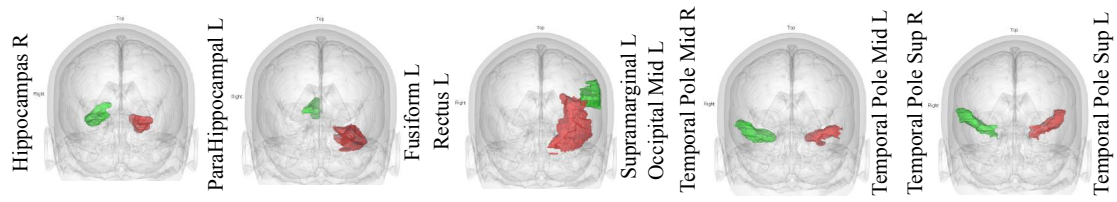


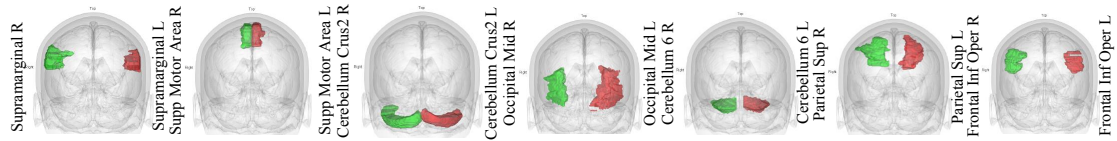
Figure 7: The Figure shows fMRI slice variation captured by one expert with semantically related keywords. We used 7 random slices from the sequence of 85 slices, to showcase the following scenarios: (i) slice sequence captured by an expert for the word “science” (top row), (ii) visualization of actual voxel activation for semantically related testing word “mathematics” (second row), (iii) visualization of predictions by the same expert for semantically related testing word “mathematics” (third row), and (iv) visualization of predicted voxels using the model trained with ridge regression (bottom row). that each expert captured distinct associations between word stimuli and corresponding brain activation in both training and testing experiments. For example, expert-1 has a higher probability for the word “science”, and the same expert displays a higher

Table 1: List of expert-wise keywords used during training, the keywords predicted during testing, and expert-wise regions of activation (ROIs) in the brain. The last row lists the common regions of activation among all the experts.

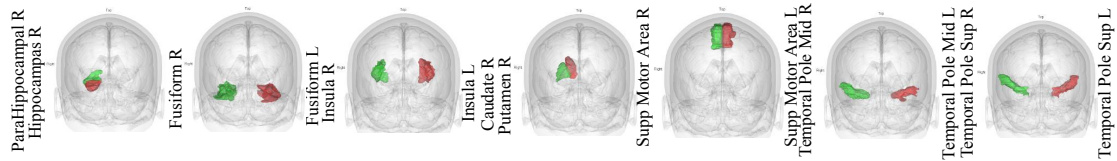
Experts	Training	Testing	Unique Brain Regions
Expert-1	argumentatively, cockroach construction, economy, gold hair, invention, jungle, land law, nation, professional, pig philosophy, science, sexy	mathematical	ParaHippocampal_L Fusiform_L, Supramarginal_L Occipital_Mid_L, Rectus_L Temporal_Pole_Sup Temporal_Pole_Mid Hippocampus_R
Expert-2	angry, bear, beat, bed, beer building, code, dedication device, dinner, dissolve doctor, election, emotion, fight garbage, help, investigation light, marriage, material mountain, relationship, shape sew, show, suspect, word	argument, art electron experiment, flow movie, residence table, tree movement	Supramarginal Occipital_Mid_L,R Cerebellum_Crus2 Cerebellum_6 Supp_Motor_Area Parietal_Sup Frontal_Inf_Oper
Expert-3	apartment, bag, bar, big, brain broken, burn, camera, computer damage, dog, dangerous, disease cook, fish, gun, extremely, feeling food, great, hurting, job, king liar, magic, news, obligation, plant play, quality, sign, skin, smart soul, sound, star, sugar, taste texture, tried, useless, wash, wear	blood, emotionally laugh, music pain, poor time	ParaHippocampal_R Fusiform_L, Fusiform_R Insula, Putamen_R Caudate_R Supp_Motor_Area Temporal_Pole_Sup Temporal_Pole_Mid Hippocampus_R
Expert-4	bird, body, challenge, do dance, deceive, dig disturb, engine, event, illness invisible, left, picture, prison read, road, seafood, usable unaware, war, weather, willingly	applause, counting spoke	Cerebellum_6, Cerebellum_8 Cerebellum_3, Thalamus Putamen_L,R, Caudate_L,R Paracentral_Lobule_L ParaHippocampal_L Occipital_Mid_L,R Supp_Motor_Area
Expert-5	ability, accomplished, business ball, charming, charity, clothes crazy, delivery, dessert, driver impress, ignorance, kindness lady, level, mechanism, money medication, noise, personality plan, pleasure, reaction religious, sad, ship, smiling solution, stupid, successful tool, weak, vacation	attitude, carefully collection, deliberately dressing, elegance protection, sell silly, sin student, team toy, trial typical	Cerebellum_6 Parietal_Sup Occipital_Mid_L,R Temporal_Pole_Mid Temporal_Pole_Sup
Angular_L,R, Lingual_L,R, Precentral_L,R, Postcentral_L,R, Cuneus_L,R Frontal_Sup_L,R, Frontal_Mid_L,R, Precuneus_L,R Cerebellum_Crus_1L,1R, Temporal_Sup_L,R, Temporal_Mid_L,R			



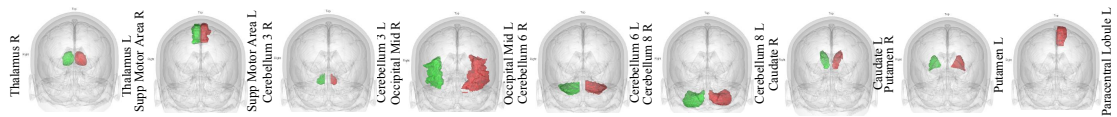
(a) Expert-1 ROIs



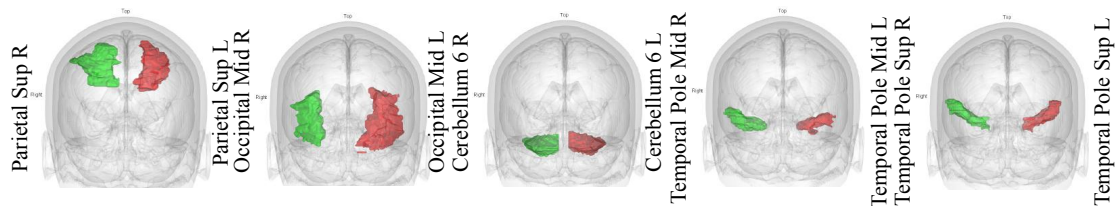
(b) Expert-2 ROIs



(c) Expert-3 ROIs



(d) Expert-4 ROIs



(e) Expert-5 ROIs

Figure 8: Expert-wise specialization in activation of regions of interest (ROIs) in the brain

probability for the test word “mathematical.” We have shown the actual brain responses for the word “science”, “mathematics” and predicted brain activation for the test word “mathematics” in Figure 7. As shown in Figure 7, we observe that the similarities between ground truth and cortical brain responses from MoRE-based encoding model are better with a near-perfect recall. In contrast, some of the voxel intensity values predicted by the ridge regression model are very negligible in critical brain regions.

We also identified the brain regions which are associated with words in each expert. We considered voxels with high activation, that is, those with intensity values more significant than a threshold (= mean) and discarded the remaining voxels with low activation values. We generated a matrix of size [#No of words in the expert \times Brain ROIs (regions which corresponding to the activated voxels)] for each expert. For example, we can see from Table 1 that Expert-1 captured 16 words in training (with 116 corresponding ROIs), yielding a matrix of size 16×116). In order to identify the ROIs associated with each expert, we applied principal component analysis (PCA) on the above matrix (#words \times regions) and extracted principal components (PCs) with a maximum explained variance ratio of 90%. This result would also enable us to identify the most critical variables in the original feature space that have a maximal contribution to the essential PCs. While brain regions such as “Angular_L,R”, “Lingual_L,R”, “Precentral_L,R”, “Postcentral_L,R”, “Cuneus_L,R”, “Frontal_Sup_L,R”, “Frontal_Mid_L,R”, “Precuneus_L,R”, “Cerebellum_Crus_1L,1R”, “Temporal_Sup_L,R”, and “Temporal_Mid_L,R” (listed in the last row of Table 1) are commonly activated among all the experts, there are unique regions captured by experts as shown in Table 1. The common ROIs seem to be related generally to visual-spatial

processing, sensory processing, attention, etc. that seem to be shared for all the words and may be related to the processing of the visual stimulus presented along with the lexical input (word).

Observations from Table 1 that the experts correspond to distinct (specialized) ROIs based on joint learning of semantic aspect of the word stimulus and the associated brain regions related to the meaning of the word. This aspect can be observed in all the experts, especially in the set of words that have a close correspondence between training and test conditions. Similarly, it can also observe that the ROIs activated are known from previous studies to have compatibility with the semantics.

Cortical areas associated with movement such as the Supplementary Motor Area, Cerebellum, Putamen, Caudate seem to be active in Expert 4 that seems to code for action words such as “read”, “spoke”, noun-verb co-occurrences such as “event-spoke”, “do dance”, “dig”, “applause”, “counting”, etc (Pulvermüller, 2013; Houk et al., 2007).

It appears that Expert 3 codes for body recognition related words such as “brain”, “skin”, and “disease”, face recognition words such as “laugh”, “emotions”, “feelings”, and “soul”, color-related words “texture”, etc. The brain activation in the Fusiform gyrus that lies between the Parahippocampal gyrus and the Lingual gyrus medially seem to be compatible with face processing (Weiner and Zilles, 2016; Bogousslavsky et al., 1987).

Expert 5 codes for abstract words such as ability, pleasure, plan, the brain activation in the polar regions of the temporal lobe known for involvement in higher-order language comprehension seems compatible. Similar correspondences can be seen in several other experts. Although, as can be seen from Table 1 that some words that the

experts seem to code for are unrelated, by and large, MoRE model seems to succeed in capturing associations between word features and relevant brain activation.

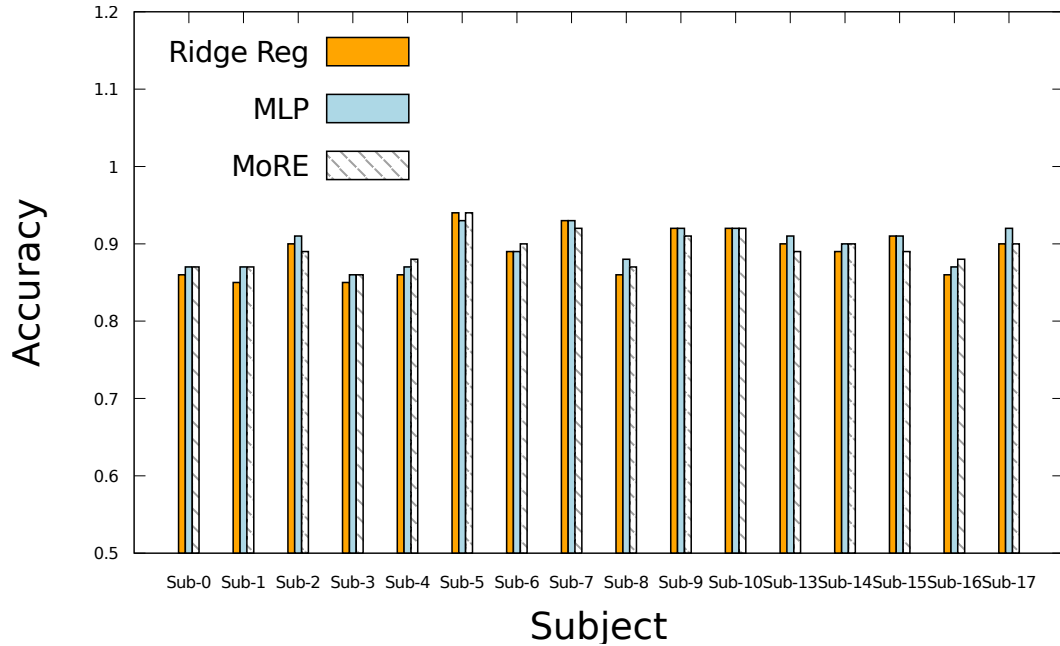


Figure 9: Comparison of accuracy of i) ridge regression model, ii) multi-layer perceptron and, iii) mixture of regression experts. The individual models built for each of the 17 participants shown here.

Figure 8 showcases expert-wise specialization in the regions of activation (ROIs) in the brain. Here, we depict slices from the coronal section of the brain, indicating the voxels corresponding to unique brain regions activated by each expert. MoRE models seem to learn the association between brain regions and the semantic meaning of the words. To assess the similarity between actual and predicted brain responses, we compared the intensity of the voxels greater than a threshold ($= \text{mean} + \text{std}$) using corresponding voxel coordinates. Figure 9 compares the performance of baseline ridge regression model, multi-layer perceptron (MLP), and the proposed MoRE model. The

proposed MoRE model matches the accuracy scores of the existing linear & non-linear models, from Figure 7, we observe that similarities between ground truth and cortical brain responses from MoRE-based encoding model are better with a near-perfect estimation of brain activation.

5.2 Stimulus Presentation of target Word and a Related Word Cloud

In this experiment, we used brain activations from paradigm-3 of experiment-1, where word cloud has shown along with the concept word to the participants. We similarly trained this model as described in Section 5.1.

Table 2 shows the unique brain regions activated in five different experts. ROIs activated commonly across all the experts are listed in the last row in Table 2. These areas seem to be related generally to visual-spatial processing, sensory processing, attention, etc. that seem to be common for all the words observed in the word+picture model shown in Table 1. Interestingly, it can observe from both Tables 1 and 2 that the model trained on word+picture discriminates all the words associated with brain regions better compared to the other model trained using the word cloud. The visual input rather than the semantic context seems to give rise to better associative learning. Anderson et al (Anderson et al., 2017) made a similar distinction between concrete and abstract nouns where visual input seemed to enhance accuracy for concrete nouns, whereas semantic models facilitate abstract nouns.

Table 2: Results from the *target word + word cloud condition*. Expert-wise keywords used during training, the keywords predicted during testing, and expert-wise regions of activation in the brain are shown. The last row lists common regions activated across all the experts.

Experts	Training	Testing	Unique Brain Regions
Expert-1	charming, damage, dessert, lady medication, smart stupid, vacation	attitude, dressing laugh, protection, typical	ParaHippocampal_L,R Hippocampus_L,R Cerebellum_4.5_L Cerebellum_6_L,R,8_L,R Supp_Motor_Area_R Putamen_L, Thalamus_R
Expert-2	angry, business, clothes, code computer, dedication, device driver, emotion, garbage, gun magic, noise, obligation personality, pleasure, reaction religious, sad, shape, ship smiling, successful, useless, wash	collection, elegance flow, movement toy	Supp_Motor_Area_L,R Cerebellum_8_L,R Cerebellum_6_L,R Occipital_Mid_L Caudate_L,R Frontal_Inf_Oper_R
Expert-3	apartment, argumentatively, bar bear, beat, bed, beer, big, bird body, brain, burn, building, camera challenge, charity, cook, cockroach construction, dance, disease dissolve, dinner, disease, disturb doctor, dog, economy, election engine, fight, fish, food, gold hair, illness, invention, invisible investigation, job, jungle, king law, liar, land, left, marriage material, mountain, news, nation plant, play, picture, philosophy prison, professional, quality, road relationship, science, seafood, sew show, sign, solution, sound, star sugar, taste, texture, tried war, wear, weather	applause, art argument, blood electron, emotionally experiment, mathematical movie, music pain, poor residence, spoke table, team tree, trial	Supp_Motor_Area_L,R Insula_L Cingulum_Ant_L,R Lingual_L,R Fusiform_R Frontal_Inf.Orb_L,R Rectus_L Cerebellum_8_L,R Cerebellum_6_L,R
Expert-4	ability, bag, ball, broken, do crazy, dangerous, delivery, dig extremely, event, feeling, great hurting, help, ignorance ,impress kindness, light, mechanism, money pig, plan, read, sexy, skin soul, suspect, tool, usable, unaware weak, willingly, word	carefully, counting deliberately, sell silly, sin time	Insula_L,R Cingulum_Ant_R Lingual_L,R Parietal_Sup_R Frontal_Inf_Tri_L,R Lingual_L,R Occipital_Mid_L Frontal_Inf.Orb_R
Expert-5	level, accomplished, deceive	student	Temporal_Mid_L,R Cingulum_Mid_R Parietal_Sup_L
Angular_L,R, Precentral_L,R, Postcentral_L,R, Cuneus_L,R Frontal_Sup_L,R, Frontal_Mid_L,R, Precuneus_L,R Cerebellum_Crus_1L,1R, Temporal_Sup_L,R, Temporal_Mid_L,R			

Table 3: MoRE prediction results for unknown words. The last row lists the common regions activated across all the experts.

Unknown Words	(Highlighted Expert)	(Related Words)	Brain Regions
Physics	Expert-1	Science, Mathematics	ParaHippocampal_L Fusiform_L, Supramarginal_L Occipital_Mid_L, Rectus_L
Lunch	Expert-2	Dinner	Supp_Motor_Area Supramarginal Frontal_Inf_Oper
Generous	Expert-5	Kindness, Charity	Temporal_Pole_Mid Temporal_Pole_Sup
Cat	Expert-5	NA	Cerebellum_6 Occipital_Mid_L,R Cerebellum_Crus_1L,1R
Angular_L,R, Precentral_L,R, Postcentral_L,R, Cuneus_L,R Frontal_Sup_L,R, Frontal_Mid_L,R, Precuneus_L,R Cerebellum_Crus_1L,1R, Temporal_Sup_L,R, Temporal_Mid_L,R			

5.3 ROI Prediction for Unknown Words

To measure the efficacy of our proposed MoRE model for the word+picture condition, we tried to predict the brain regions for unknown words, i.e., those that are not present in the dataset. We chose four different words such as “physics”, “lunch”, “generous”, and “cat” which are semantically related to words in the existing dataset but not explicitly given while training, model prediction results are displayed in Table 3. For the word “physics”, MoRE model chose expert-1 with higher probability among the five experts and expert-1 earlier captured the words science and mathematics in training & testing,

respectively as shown in Table 1. Except for the word “cat”, the remaining three words are correctly captured by the corresponding experts. The results of this unknown-word experiment give credence to our hypothesis that learning functional differentiation (or specialization) while achieving comparable overall accuracy can be implemented with the mixture of regression experts (MoRE) framework.

6 Conclusion

In this paper, we present a mixture of experts based model (ExpertoCoder) where a group of experts captures brain activity patterns related to particular regions of interest (ROIs) and also show semantic discrimination across different experts. Different from previous works, the underlying model depicts that each expert trains on particular brain regions of interest (set of voxels that are significantly activated) based on the semantic category of words that are represented by the model. Various experiments demonstrated the efficacy and validity of the proposed approach. Notably, the last experiment on unknown words demonstrates the power of such encoding models that learn a joint association between semantics from linguistic representation and brain responses. These models can potentially predict the brain response corresponding to new words.

In future, we plan to experiment on Spatio-temporal fMRI datasets and identify the number of experts using Bayesian Information Criterion (BIC), with a primary focus on the hierarchical mixture of experts at slice-level instead of voxel-level predictions at each instance.

References

- Abnar, S., Ahmed, R., Mijnheer, M., and Zuidema, W. (2018). Experiential, distributional and dependency-based word embeddings have complementary roles in decoding brain activity. In *Proceedings of the 8th Workshop on Cognitive Modeling and Computational Linguistics (CMCL 2018)*, pages 57–66.
- Anderson, A. J., Kiela, D., Clark, S., and Poesio, M. (2017). Visually grounded and textual semantic models differentially decode brain activity associated with concrete and abstract nouns. *Transactions of the Association for Computational Linguistics*, 5:17–30.
- Benjamin, A. S., Fernandes, H. L., Tomlinson, T., Ramkumar, P., VerSteeg, C., Miller, L., and Kording, K. P. (2017). Modern machine learning far outperforms glms at predicting spikes. *BioRxiv*, page 111450.
- Bogousslavsky, J., Miklossy, J., Deruaz, J.-P., Assal, G., and Regli, F. (1987). Lingual and fusiform gyri in visual processing: a clinico-pathologic study of superior altitudinal hemianopia. *Journal of Neurology, Neurosurgery & Psychiatry*, 50(5):607–614.
- Chang, K.-m. K., Mitchell, T., and Just, M. A. (2011). Quantitative modeling of the neural representation of objects: how semantic feature norms can account for fmri activation. *NeuroImage*, 56(2):716–727.
- Craddock, R. C., James, G. A., Holtzheimer III, P. E., Hu, X. P., and Mayberg, H. S. (2012). A whole brain fmri atlas generated via spatially constrained spectral clustering. *Human Brain Mapping*, 33(8):1914–1928.

- Devlin, J., Chang, M.-W., Lee, K., and Toutanova, K. (2018). Bert: Pre-training of deep bidirectional transformers for language understanding. *arXiv preprint arXiv:1810.04805*.
- Di Liberto, G. M., OSullivan, J. A., and Lalor, E. C. (2015). Low-frequency cortical entrainment to speech reflects phoneme-level processing. *Current Biology*, 25(19):2457–2465.
- Dietterich, T. G. (2000). Ensemble methods in machine learning. In *International Workshop on Multiple Classifier Systems*, pages 1–15. Springer.
- Dumoulin, S. O. and Wandell, B. A. (2008). Population receptive field estimates in human visual cortex. *NeuroImage*, 39(2):647–660.
- Eavani, H., Hsieh, M. K., An, Y., Erus, G., Beason-Held, L., Resnick, S., and Davatzikos, C. (2016). Capturing heterogeneous group differences using mixture-of-experts: Application to a study of aging. *Neuroimage*, 125:498–514.
- Fernandino, L., Humphries, C. J., Seidenberg, M. S., Gross, W. L., Conant, L. L., and Binder, J. R. (2015). Predicting brain activation patterns associated with individual lexical concepts based on five sensory-motor attributes. *Neuropsychologia*, 76:17–26.
- Gonsalves, B. D. and Cohen, N. J. (2010). Brain imaging, cognitive processes, and brain networks. *Perspectives on Psychological Science*, 5(6):744–752.
- Güçlü, U. and van Gerven, M. A. (2017). Increasingly complex representations of

- natural movies across the dorsal stream are shared between subjects. *NeuroImage*, 145:329–336.
- Han, K., Wen, H., Shi, J., Lu, K.-H., Zhang, Y., and Liu, Z. (2018). Variational autoencoder: An unsupervised model for modeling and decoding fmri activity in visual cortex. *BioRxiv*, page 214247.
- Houk, J. C., Bastianen, C., Fansler, D., Fishbach, A., Fraser, D., Reber, P. J., Roy, S., and Simo, L. S. (2007). Action selection and refinement in subcortical loops through basal ganglia and cerebellum. *Philosophical Transactions of the Royal Society B: Biological Sciences*, 362(1485):1573–1583.
- Jordan, M. I. and Xu, L. (1995). Convergence results for the em approach to mixtures of experts architectures. *Neural Networks*, 8(9):1409–1431.
- Kass, R. E. and Raftery, A. E. (1995). Bayes factors. *Journal of the American Statistical Association*, 90(430):773–795.
- Kay, K. N., Naselaris, T., Prenger, R. J., and Gallant, J. L. (2008). Identifying natural images from human brain activity. *Nature*, 452(7185):352.
- Kim, S., Smyth, P., and Stern, H. (2010). A bayesian mixture approach to modeling spatial activation patterns in multisite fmri data. *IEEE Transactions on Medical Imaging*, 29(6):1260–1274.
- Kording, K. P., Benjamin, A., Farhoodi, R., and Glaser, J. I. (2018). The roles of machine learning in biomedical science. In *Frontiers of Engineering: Reports on Leading-Edge Engineering from the 2017 Symposium*. National Academies Press.

- Mahmoudi, A., Takerkart, S., Regragui, F., Boussaoud, D., and Brovelli, A. (2012). Multivoxel pattern analysis for fmri data: a review. *Computational and Mathematical Methods in Medicine*, 2012.
- Mesgarani, N., Cheung, C., Johnson, K., and Chang, E. F. (2014). Phonetic feature encoding in human superior temporal gyrus. *Science*, 343(6174):1006–1010.
- Mikolov, T., Sutskever, I., Chen, K., Corrado, G. S., and Dean, J. (2013). Distributed representations of words and phrases and their compositionality. In *Advances in Neural Information Processing Systems*, pages 3111–3119.
- Mitchell, T. M., Shinkareva, S. V., Carlson, A., Chang, K.-M., Malave, V. L., Mason, R. A., and Just, M. A. (2008). Predicting human brain activity associated with the meanings of nouns. *Science*, 320(5880):1191–1195.
- Naselaris, T., Kay, K. N., Nishimoto, S., and Gallant, J. L. (2011). Encoding and decoding in fmri. *NeuroImage*, 56(2):400–410.
- Oota, S. R., Manwani, N., and Bapi, R. S. (2018). fmri semantic category decoding using linguistic encoding of word embeddings. In *International Conference on Neural Information Processing*, pages 3–15. Springer.
- Oota, S. R., Rowtula, V., Gupta, M., , and Bapi, R. S. (2019). Stepencog: A convolutional lstm autoencoder for near-perfect fmri encoding. In *2019 International Joint Conference on Neural Networks (IJCNN)*, pages 4564–4570. IEEE.
- Palatucci, M., Pomerleau, D., Hinton, G. E., and Mitchell, T. M. (2009). Zero-shot

- learning with semantic output codes. In *Advances in Neural Information Processing Systems*, pages 1410–1418.
- Paninski, L., Pillow, J., and Lewi, J. (2007). Statistical models for neural encoding, decoding, and optimal stimulus design. *Progress in Brain Research*, 165:493–507.
- Pennington, J., Socher, R., and Manning, C. (2014). Glove: Global vectors for word representation. In *Proceedings of the 2014 Conference on Empirical Methods in Natural Language Processing (EMNLP)*, pages 1532–1543.
- Pereira, F., Lou, B., Pritchett, B., Ritter, S., Gershman, S. J., Kanwisher, N., Botvinick, M., and Fedorenko, E. (2018). Toward a universal decoder of linguistic meaning from brain activation. *Nature Communications*, 9(1):963.
- Pulvermüller, F. (2013). How neurons make meaning: brain mechanisms for embodied and abstract-symbolic semantics. *Trends in Cognitive Sciences*, 17(9):458–470.
- Rowtula, V., Oota, S., Gupta, M., and Surampudi, B. R. (2018). A deep autoencoder for near-perfect fmri encoding.
- Weiner, K. S. and Zilles, K. (2016). The anatomical and functional specialization of the fusiform gyrus. *Neuropsychologia*, 83:48–62.
- Wen, H., Shi, J., Chen, W., and Liu, Z. (2018). Transferring and generalizing deep-learning-based neural encoding models across subjects. *NeuroImage*, 176:152–163.
- Wen, H., Shi, J., Zhang, Y., Lu, K.-H., Cao, J., and Liu, Z. (2017). Neural encoding and decoding with deep learning for dynamic natural vision. *Cerebral Cortex*, 28(12):4136–4160.

Yamins, D. L., Hong, H., Cadieu, C. F., Solomon, E. A., Seibert, D., and Di-Carlo, J. J. (2014). Performance-optimized hierarchical models predict neural responses in higher visual cortex. *Proceedings of the National Academy of Sciences*, 111(23):8619–8624.

Yao, B., Walther, D., Beck, D., and Fei-Fei, L. (2009). Hierarchical mixture of classification experts uncovers interactions between brain regions. In *Advances in Neural Information Processing Systems*, pages 2178–2186.

7 Appendix

Here, we display the voxels corresponding to the unique brain regions activated by each expert in a slice-wise format. in 10.

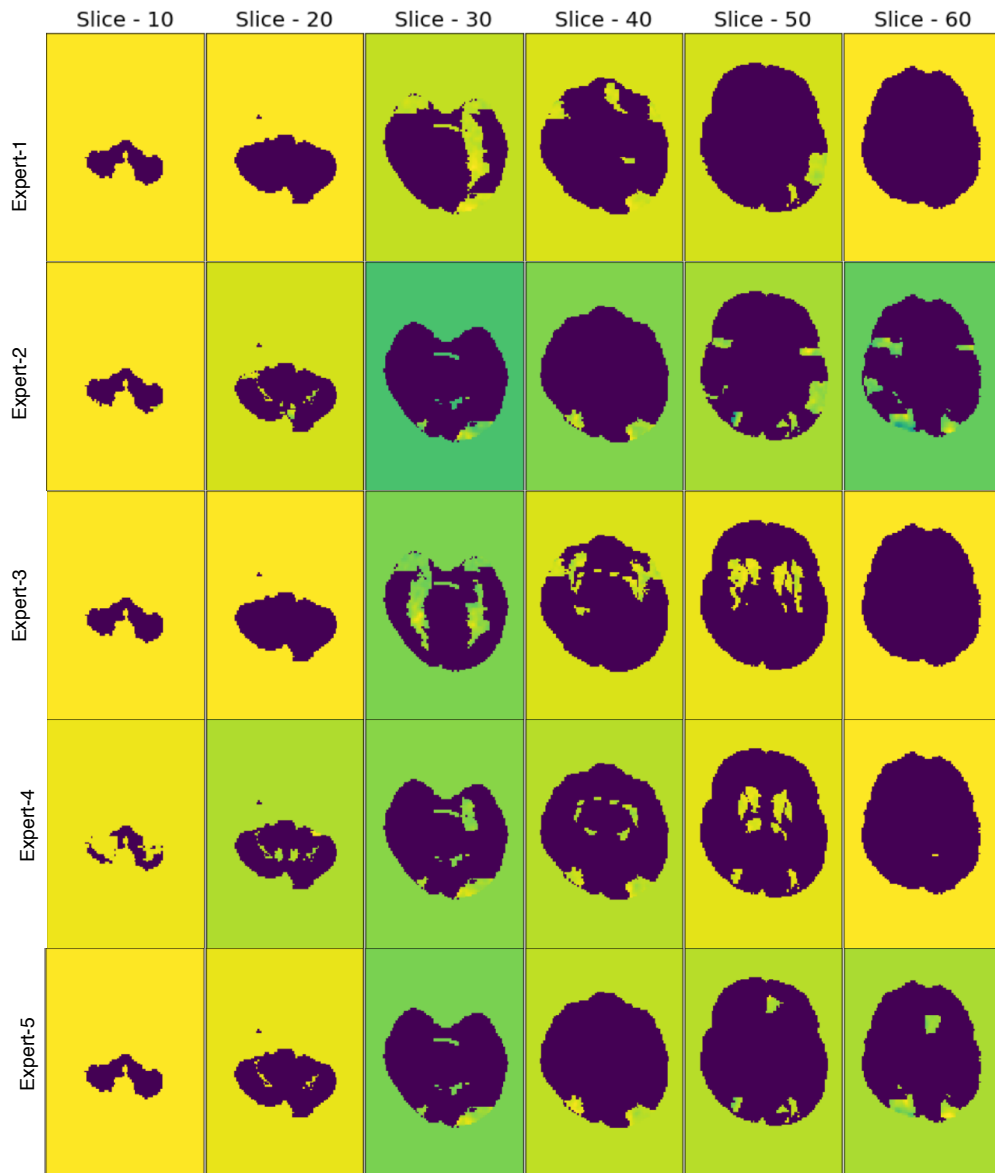


Figure 10: The figure captures expert-wise regions of activation in the brain. The predicted voxel values are converted into 85 2D slices and 6-slices per expert are displayed in the image.